

Enhanced magnetoelectric effect in longitudinal-transverse mode Terfenol-D/Pb(Mg_{1/3}Nb_{2/3})O₃–PbTiO₃ laminate composites with optimal crystal cut

Yaojin Wang,^{1,2,3} Siu Wing Or,^{2,a)} Helen Lai Wa Chan,² Xiangyong Zhao,¹ and Haosu Luo¹

¹State Key Laboratory of High Performance Ceramics and Superfine Microstructure, Shanghai Institute of Ceramics, Chinese Academy of Sciences, 215 Chengbei Road, Jiading, Shanghai 201800, People's Republic of China

²Department of Applied Physics, The Hong Kong Polytechnic University, Hung Hom, Kowloon, Hong Kong

³Graduate School of the Chinese Academy of Sciences, Beijing 10039, People's Republic of China

(Received 10 April 2008; accepted 15 April 2008; published online 23 June 2008)

Magnetoelectric (ME) laminate composite consisting of optimal crystal cut thickness-polarized piezoelectric 0.7Pb(Mg_{1/3}Nb_{2/3})O₃–0.3PbTiO₃ (PMN-PT) single crystal and the length-magnetized magnetostrictive Tb_{0.3}Dy_{0.7}Fe_{1.92} (Terfenol-D) alloy has been fabricated. The cut optimization of PMN-PT crystal greatly enhances the longitudinally magnetized-transversely polarized (*L-T*) mode ME effect, which has a superior ME voltage coefficient α_E of ~ 3.02 V/cm Oe in low frequency band. Near the resonance frequency of 95 kHz, the coefficient dramatically increases and reaches the maximized value of 33.2 V/cm Oe, which is almost two times larger than the previously reported $\langle 001 \rangle$ -oriented PMN-PT crystal based *L-T* mode laminate composite. © 2008 American Institute of Physics. [DOI: 10.1063/1.2943267]

I. INTRODUCTION

The magnetoelectric (ME) effect is the polarization P response to an applied magnetic field H , and the converse ME effect is a magnetization M response to an applied electric field E .¹ In the past decades, considerable research efforts have been put on the ME effect, first in single-phase materials, then in two-phase bulk composites, and lately in two-/three-phase laminate composites.^{2–9} The magnetic-to-electric field conversion in ME composite is a magnetoelasto-electric coupling.³ The ME coupling in laminate composite is realized by a stress mediated interaction between the magnetostrictive phase (or ferromagnet) and the piezoelectric (or ferroelectric) phase, which is often referred to as a multiferroic composite.⁴ Some simple architecturally engineered nanostructured composites, such as CoFe₂O₄ nanopillars in a BaTiO₃ matrix, have also recently been reported.⁵ It seems that these nanocomposites should have potential for high ME coupling because the two phase materials have a more intimate contact in nanodimension. But these nanostructured composites suffer from the drawback that the magnetostrictive and piezoelectric effects are dramatically decreased in nanodimension due to substrate's clamping effect.⁶ To date, it is known that laminated composites of piezoelectric 0.7Pb(Mg_{1/3}Nb_{2/3})O₃–0.3PbTiO₃ (PMN-PT) single crystal and magnetostrictive Tb_{0.3}Dy_{0.7}Fe_{1.92} (Terfenol-D) alloy possess superior ME effect and ultrahigh magnetic field sensitivity due to their greater product effect of the piezoelectric effect and the magnetostrictive effect.⁷ However, the orientation of piezoelectric PMN-PT single crystal was out of consideration in previous studies. Actually, based on the

working principle of *L-T* mode laminate composite, the Terfenol-D mainly vibrates longitudinally when the applied magnetic field is along the length direction. Due to the mechanical coupling, the PMN-PT single crystal has to vibrate synchronously along the length direction and generates electric charge along the thickness direction. So the piezoelectric coefficient d_{31} and electromechanical coupling factor k_{31} should contribute greatly to the ME effect.⁷ Consequently, designing new optimal cut-types in the single crystal piezoelectric phase to produce optimized transverse piezoelectric performance is a new method to enhance the applications of ME effect.

In this paper, we have developed an *L-T* mode ME laminate composite by sandwiching a special-oriented piezoelectric PMN-PT single crystal between two longitudinally magnetized magnetostrictive Terfenol-D plates.

II. EXPERIMENTS

A. Structure and fabrication

Figure 1 shows schematic diagram of the proposed sand-

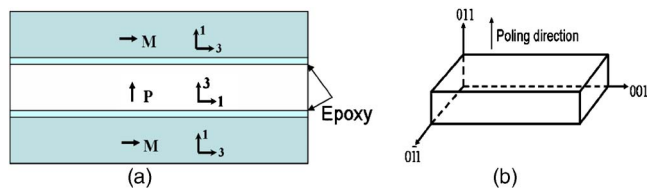


FIG. 1. (Color online) (a) Schematic diagram of the proposed magnetostrictive/piezoelectric laminated composites. The arrows designate the magnetization and polarization directions, respectively. (b) The newly designed special-oriented PMN-PT single crystal. The $\langle 001 \rangle$, $\langle 0\bar{1}1 \rangle$, and $\langle 011 \rangle$ crystallographic axes are oriented in the length, width, and thickness directions, respectively.

^{a)}Author to whom correspondence should be addressed. Electronic mail: apswor@polyu.edu.hk.

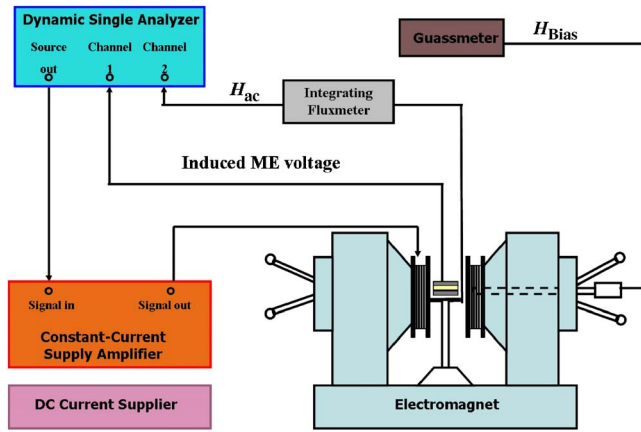


FIG. 2. (Color online) Schematic diagram of the ME measurement setup.

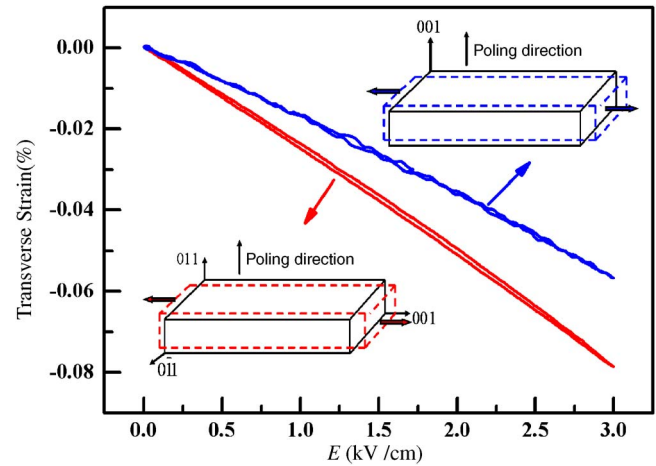
wiched composite structure with the ME effect and the optimal cut-type of PMN-PT plate. The high quality PMN-PT single crystal was grown directly from the melt by modified Bridgman technique.¹⁰ The as-grown single crystals were oriented along $\langle 001 \rangle$, $\langle 011 \rangle$, and $\langle 0\bar{1}1 \rangle$ directions using an x-ray diffraction meter, and then diced to prepare samples with the crystal cut and dimensions of $12\langle 001 \rangle^L \times 6\langle 0\bar{1}1 \rangle^W \times 1\langle 011 \rangle^T \text{ mm}^3$ (L : length, W : width, T : thickness). It has been shown in our previous work that PMN-PT plates, with this specially cut and poled along the $\langle 011 \rangle$ thickness direction, possess ultrahigh transverse piezoelectric performance, i.e., ultrahigh thickness direction voltage response to length direction strain deformation.¹¹ The Terfenol-D plates were commercially supplied (Baotou Research Institute of Rare Earth, China) with the same dimensions as the PMN-PT plate and with the length direction along the $[112]$ direction, which is the highly magnetostrictive crystallographic axis and the magnetization (M) was relatively easy to achieve.¹²

B. Measurement setup and procedure

The ME properties of the laminate composite were characterized at room temperature and zero stress bias using an in-house automated measurement system¹³ shown in Fig. 2. The ME voltages (V) induced in the composites were measured as a function of ac magnetic field (H_{ac}), dc magnetic bias (H_{bias}), and ac magnetic field frequency (f) in the ranges of 10^{-7} – 10^{-3} T, 0–1200 Oe, and 1–100 kHz, respectively. H_{ac} was provided by Helmholtz coils driven by a dynamic signal analyzer (Ono Sokki CF5220) via a constant-current supply amplifier (AE Techron 7572). H_{bias} was supplied by a water-cooled, U-shaped electromagnet (Mytem PEM-8005K) controlled by a dc current supply (Sorensen DHP200-15). H_{ac} and H_{bias} were monitored *in situ* by a pick-up coil connected to an integrating fluxmeter (Walker MF-10D) and a Guassmeter (F. W. Bell 7030), respectively. All quantities were sampled and recorded by the dynamic signal analyzer and stored in a computer.

III. RESULTS AND DISCUSSION

It is well known that PMN-PT single crystal has superior piezoelectric effect and electromechanical coupling perfor-

FIG. 3. (Color online) Strain vs E -field (unipolar) curves in the $\langle 001 \rangle$ -oriented and newly designed cut-type PMN-PT crystals.

mance. However, the piezoelectric effect of PMN-PT is anisotropic, depending significantly on the crystal cut type and the poling direction. Consequently, optimization of the crystal cut and poling processing of PMN-PT single crystals should be considered to produce optimal piezoelectric performance for different piezoelectric resonator modes in versatile applications. Figure 3 shows the electric-field induced strain patterns for the $\langle 001 \rangle$ -oriented and newly designed cut-type 0.70PMN-0.30PT crystal, respectively, using a unipolar field with amplitude of $E < 3$ kV/cm and frequency of 0.2 Hz. From the slope of the plot, the piezoelectric coefficients of d_{31} were determined. The k_{31} was determined using the resonance-antiresonance technique by a HP 4194A impedance analyzer following the IEEE standards, and d_{33} is directly measured by a quasistatic Berlincourt d_{33} meter (50 Hz) (see Table I). From the comparison in Table I, it is obviously observed that the newly designed cut-type PMN-PT crystal is much superior for transverse mode application than the $\langle 001 \rangle$ -oriented one.

The ME voltage coefficient α_E , defined as $|dE/dH_{ac}|$, of the as-prepared crystal cut optimized laminate composite was then measured for various H_{bias} at H_{ac} of 1 Oe peak and f of 1 kHz, as shown in Fig. 4. α_E initially increases rapidly with H_{bias} and reaches a maximum value of ~ 3.02 V/cm Oe at an optimal H_{bias} of 400 Oe, then decreases with increasing H_{bias} . In addition, the laminated composite has almost a linear response to H_{bias} in the range of $0 < H_{bias} < 200$ Oe. Correspondingly, the relationship of the laminated composite can be used to detect small dc magnetic field.⁸

Figure 5 illustrates the induced ME voltage V across the PMN-PT plate as a function of applied H_{ac} over the range of $10^{-7} < H_{ac} < 10^{-3}$ T at $f = 1$ kHz. It is clear that V has an

TABLE I. Piezoelectric parameters for $\langle 001 \rangle$ -oriented and newly designed cut-type PMN-PT crystals.

	d_{31} ($\times 10^{-12}$ C/N)	d_{33} ($\times 10^{-12}$ C/N)	k_{31}	$\varepsilon_{33}^T/\varepsilon_0$
$\langle 001 \rangle$ -oriented	-1126	2420	0.62	4276
$[001]^L \times [\bar{1}10]^W \times [110]^T$ -oriented	-2645	2060	0.95	6200

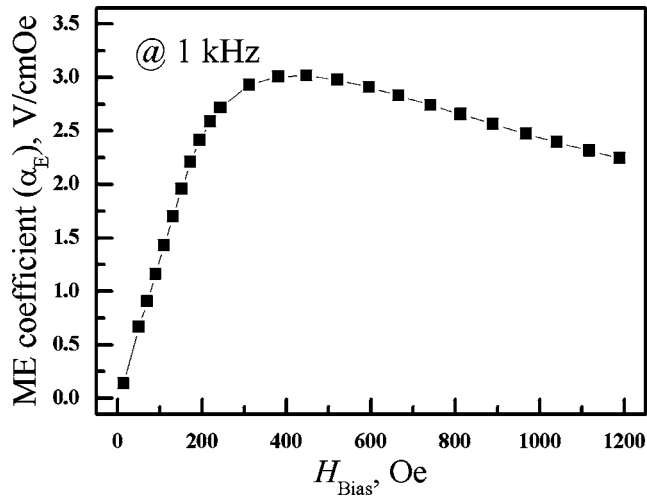


FIG. 4. ME voltage coefficient α_E of the new laminated composite as a function of H_{bias} . These data were taken using $H_{\text{ac}}=1$ Oe peak at $f=1$ kHz.

excellent linear response to H_{ac} in the whole measured range for various H_{bias} . A higher detection sensitivity of 10^{-10} – 10^{-11} T could be obtained if shielding magnetic noise could be adopted and composite fabrication could be improved.⁷ From the slope of the plot, the ME voltage coefficient α_E for various H_{bias} can also be determined, which coincides reasonably well with α_E versus H_{bias} , as shown in Fig. 4.

The dependence of α_E on f at various H_{bias} is shown in Fig. 6(a). It is noted that no remarkable dispersion of α_E is observed for all cases apart from the variations associated with the ME resonances. The largest α_E is observed at $H_{\text{bias}}=400$ Oe for the whole frequency range. In particular, the maximal resonance α_E located at the ME resonances frequency (f^{MER}) of 95.25 kHz under this optimal H_{bias} is as large as 33.2 V/cm Oe. This resonance α_E at f^{MER} is over 13 times larger than its nonresonance α_E of ~ 3.02 V/cm Oe. Figure 6(b) shows H_{bias} dependence of f^{MER} and α_E at f^{MER} . The results clearly demonstrate that the variation of α_E at f^{MER} is similar to the α_E at nonresonant frequency, as shown in Fig. 4. However, f^{MER} decreases with increasing H_{bias} ,

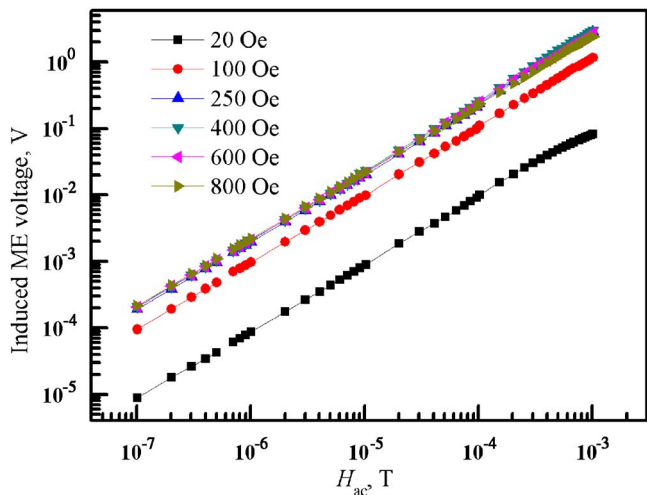


FIG. 5. (Color online) Induced ME voltage V as a function of applied H_{ac} over the range of $10^{-7} < H_{\text{ac}} < 10^{-3}$ T at $f=1$ kHz for various H_{bias} .

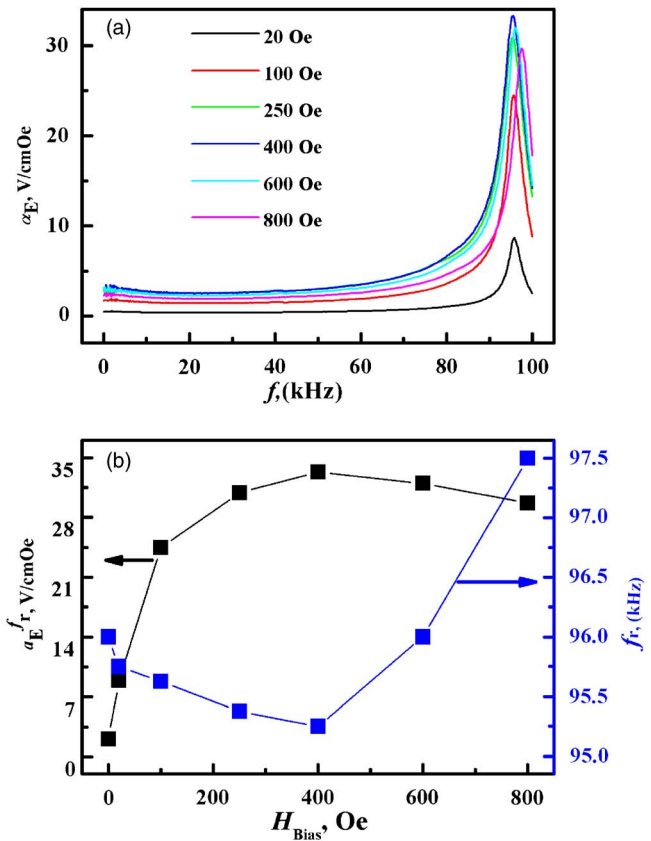


FIG. 6. (Color online) (a) Frequency response of ME voltage coefficient α_E for various H_{bias} , and (b) H_{bias} dependence of ME voltage coefficient at ME resonances α_E^{MER} and ME resonances frequency f_r .

reaching the smallest value of 95.25 kHz at $H_{\text{bias}}=400$ Oe, and then increasing with increasing H_{bias} . Physically, the initial change in both α_E (at f^{MER}) and f^{MER} with increasing H_{bias} can be explained by the H_{bias} -induced motion of the available non- 180° domain walls in the Terfenol-D plates.¹³ That is, as H_{bias} increases to the 400 Oe critical value, the compliance associated with increased deformation contribution from this non- 180° domain-wall motion is maximized, resulting in a maximum in strain (and hence α_E at nonresonant frequency and α_E at f^{MER}) and a minimum in stiffness (and hence f^{MER}). Beyond this optimal and also critical value of H_{bias} , constraining of non- 180° domain-wall motion due to interaction with H_{bias} gives rise to a decrease in strain and an increase in stiffness. It is noted that the deformation contribution from the motion of 180° domain walls is insignificant as it produces changes in magnetization without accompanying strain.⁹

IV. SUMMARY

In summary, our specially designed L - T mode ME laminate composite by sandwiching PMN-PT plate with the optimal cut type of $\langle 001 \rangle^L \times \langle 0\bar{1}1 \rangle^w \times \langle 011 \rangle^T$ between two Terfenol-D plates enhances the elastoelectric coupling in the magnetic-to-electric field conversion, which results in a significantly increased ME voltage coefficient, approximately two times larger than the previous L - T mode laminate com-

posite of $\langle 001 \rangle$ -oriented PMN-PT single crystal. This reveals a new method to enhance the ME effect of the ME composite.

ACKNOWLEDGMENTS

This work was supported by the 863 High Technology and Development Project of the People's Republic of China (2006AA03Z107), the Natural Science Foundation of China (50432030, 50777065, and 50602047), the Scientific Innovation Program of Chinese Academy of Sciences (KGCX2-YW-111-7), Shanghai Municipal Government (06DZ05016), Innovation Funds from Shanghai Institute of Ceramics of Chinese Academy of Sciences (Grant No. SCX0608), the Research Grants Council of the HKSAR Government (PolyU 5255/03E), and the Innovation and Technology Fund of the HKSAR Government (GHP/003/06).

- ¹L. D. Landau and E. Lifshitz, *Electrodynamics of Continuous Media* (Pergamon, Oxford, 1960), p. 119.
- ²V. J. Folen, G. T. Rado, and E. W. Stalder, *Phys. Rev. Lett.* **6**, 607 (1961).
- ³C. W. Nan, *Phys. Rev. B* **50**, 6082 (1994).
- ⁴G. Srinivasan, E. T. Rasmussen, J. Gallegos, R. Srinivasan, Y. I. Bokhan, and V. M. Laletin, *Phys. Rev. B* **64**, 214408 (2001).
- ⁵H. Zheng, J. Wang, S. E. Lofland, A. Ma, L. Mohaddes-Ardabili, T. Zhao, L. Salamanca-Riba, S. R. Shinde, S. B. Ogale, F. Bai, D. Viehland, Y. Jia, D. G. Schlom, M. Wuttig, A. Roytburd, and R. Ramesh, *Science* **303**, 661 (2004).
- ⁶V. M. Petrov, G. Srinivasan, M. I. Bichurin, and A. Gupta, *Phys. Rev. B* **75**, 224407 (2007).
- ⁷S. X. Dong, J. F. Li, and D. Viehland, *Appl. Phys. Lett.* **83**, 2265 (2003).
- ⁸S. X. Dong, J. Y. Zhai, J. F. Li, and D. Viehland, *Appl. Phys. Lett.* **88**, 082907 (2006).
- ⁹T. L. Li, S. W. Or, and H. L. W. Chan, *J. Magn. Magn. Mater.* **304**, 442 (2004).
- ¹⁰H. S. Luo, G. S. Xu, P. C. Wang, H. Q. Xu, and Z. W. Yin, *J. Appl. Phys.* **39**, 5581 (2000).
- ¹¹J. Peng, H. S. Luo, D. Lin, H. Q. Xu, T. H. He, and W. Q. Jin, *Appl. Phys. Lett.* **85**, 6221 (2004).
- ¹²G. Engdahl, *Magnetostrictive Materials Handbook* (Academic, New York, 2000).
- ¹³S. W. Or, T. Li, and H. L. W. Chan, *J. Appl. Phys.* **97**, 10M308 (2005).